Flow Analysis of Transverse Injection in a Typical Strut-Based Scramjet Combustor

G. Sridhar[1], E. Balasubramanian[2]. B.T.N. Sridhar[3]

[1]Research Scholar, [2]Professor
Department of Mechanical Engineering
National Institute of Technical Teachers Training and Research, Chennai, India.
balasubramanian@nitttrc.edu.in
[3]Professor, Department of Aerospace Engineering
Madras Institute of Technology, Chennai, India

***Abstract*:** In scramjet engines, combustion occurs at supersonic speeds, posing challenges to flame stabilization and fuel mixing since the flame can easily be extinguished before reaching the nozzle. Adding struts in the combustor can help slow down the main flow slightly, which aids fuel-air mixing and stabilising the flame. Transverse injection was preferred due to its mixing efficiency. In the present study, an experimental flow visualization analysis of non-reacting flow in the Scramjet combustor was conducted using air as the transverse injection medium. Visualization of transverse cold flow inside the scramjet combustor was performed with a half-swept, V-grooved strut, where the injection was tested in two positions: one in front of and one behind the strut. The position of the injector was at 30% of the strut length and was analyzed at strut angles of 0° and 20°. The secondary transverse injection was maintained at 12 bar while comparing the flow field between the plane and the V-grooved strut. The impact of secondary injection while placing the V-grooved strut was also observed under different injection pressures of 12 bar and 11 bar by maintaining the combustor inlet total pressure of 10 bar. Using a high-speed jet facility and a scramjet combustor with an exit Mach number of 2.55, the study employed air for secondary injection to simulate the effects of hydrogen in cold flow conditions. The flow visualization was done by using the Schlieren technique, while pressure measurement points marked recirculation zones and shock locations. The experimental observations showed that the grooved strut improved mixing efficiency compared to the flat strut, as indicated by a larger vorticity region seen behind the strut. The shock patterns under varied injection pressure were the same for the grooved strut configuration. The mixing of secondary fluid with the main flow of air enhanced the combustion efficiency and it was visually proven by flow visualization.

***Keywords**: Scramjet Combustor, V-Grooved Strut, Transverse Injection, Cold Flow Analysis, Flow Visualization*

I. INTRODUCTION

Struts are solid structures positioned at the injection point in combustors to improve mixing. They generate vortices in the flow and enhance the entrainment of fuel and air, leading to more efficient mixing. The numerical investigation [1] was done to study the mixing and flow field characteristics of a Straight Strut (SS) and a Tapered Strut (TS), both with a constant ramp angle and height, at free-stream Mach 2. The hydrogen and ethylene were injected transversely from the rear of the strut. The Schlieren images highlight the shock-expansion wave interaction, shock/shear layer interaction, and shock/shock interaction. In the gas flow field inside a strut-based liquid-kerosene-fueled scramjet combustor [2], the thermochemical analysis of various parameters was conducted

by comparing cross-sectional views at different longitudinal locations and the axial distribution of area-averaged properties. From the comparison of computed thrust and combustion efficiency across different cases, the study found that higher combustion efficiency does not necessarily result in higher thrust. The drag caused by the fuel injection struts plays a significant role in determining the overall performance of the scramjet combustor. Another study [3] examines the impact of fuel injection schemes on the performance of a model scramjet combustor. It concludes that injecting fuel upstream of the ramp improves fuel spread. The flow over the cavity is significantly influenced

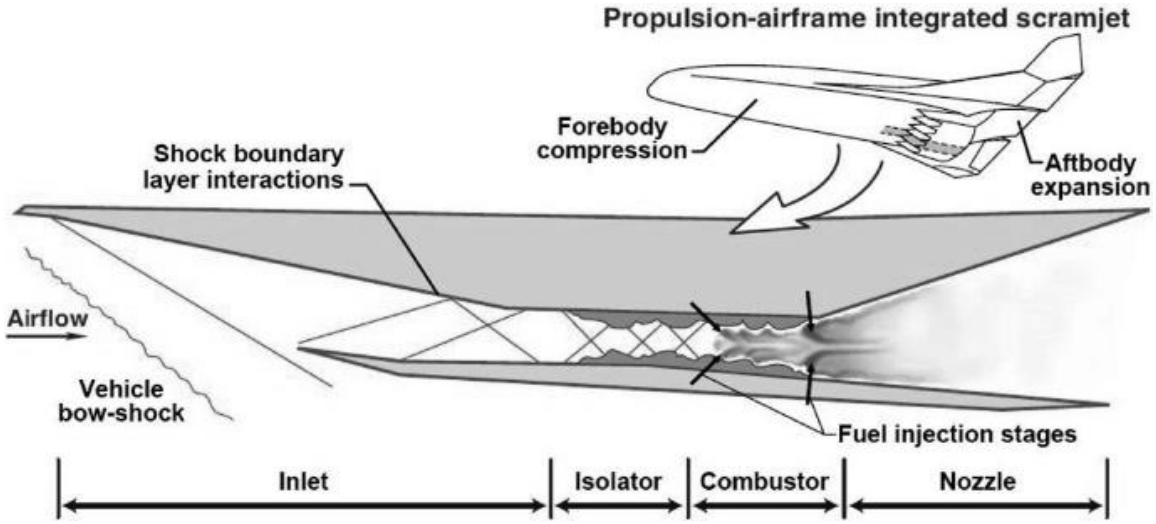

by the ramps and fuel injection between the ramps enhances fuel distribution within the combustor.

Fig. 1 The Scramjet Engine

Another study [3] examines the impact of fuel injection schemes on the performance of a model scramjet combustor. It concludes that injecting fuel upstream of the ramp improves fuel spread. The flow over the cavity is significantly influenced by the ramps and fuel injection between the ramps enhances the fuel spread within the combustor. A detailed investigation of flame characteristics [4] of scramjet combustor with a staged strut and wall ramp-based injection scheme was conducted. It focussed on the interface region between supersonic and dual-mode combustion and seems to exist in stable states at that type of combustion. They varied the equivalence ratios of both the first and second injection stages which was inferred. They have mentioned techniques for handling high temperature, long duration Schlieren system which was noted. The three-dimensional Reynolds Averaged Navier-Stokes (RANS) equations, coupled with the two-equation SST K-omega turbulence model, were employed for numerical simulation to study the mixing characteristics of transverse injection flow fields [5], combined with a micro-ramp and port hole to enhance mixing. Comparisons were made for various port hole locations with different aspect ratios. Among the tested cases, the aspect ratio of 64:1 was found to be the most efficient for injection compared to the others.

The mixing characteristics based on the traditional transverse injection technique were investigated using three-dimensional Reynolds Averaged Navier-Stokes (RANS) equations, coupled with a two-equation K-Omega shear stress transport (SST) turbulence model [6]. A symmetric cone-shaped ramp was mounted, and it was observed that stronger streamwise vorticity, generated by various mixing enhancement strategies, was the primary factor in improving mixing. However, the

study revealed that the mixing length and pressure loss at transverse velocities exhibit opposite trends as the intensity of the stream velocity varies.

The study investigated the effects of a micro-ramp on a transverse jet in supersonic crossflow using Large Eddy Simulation (LES) at Mach 2.7, employing the recycling-rescaling method to replicate the turbulent boundary layer [7]. The researchers tested under different cases for front and back jet flow, and plate jet configurations and compared their mixing efficiencies at various length-to-diameter (x/d) ratios. The results showed that the back jet was more efficient than the other two configurations for all x/d ratios. They concluded that the jet positioned behind the micro-ramp achieved significantly greater penetration. Additionally, when comparing the probability distribution of the mass fraction in the jet plume, it was observed that the main jet in the back jet easily reached the plume's centre. The influence of vortex generators in a solid scramjet was studied through direct-connect fire tests at a Mach number of 5.5 at an altitude of 23 km [8]. Hydrocarbon fuel was used in the form of a fuel-rich solid propellant. The results were compared to a benchmark configuration without vortex generators, revealing that the configurations with vortex generators significantly enhanced fuel-air mixing and stabilized combustion. The combustion efficiency [9] reached 0.60 with vortex generators, compared to only 0.11 in the benchmark case. Additionally, the ignition time delay was significantly reduced in the presence of vortex generators compared to the benchmark configuration. This study examines the impact of transverse flow using a notch-type strut, which features a V-shaped notch inclined at a specific angle from the middle to the end. This design generates oblique shocks [10] on either side of the strut, thereby enhancing the degree of mixing of fuel and air. This study [11] also made a numerical analysis on the same conditions and calculated the amount of vorticity generated at the aft surface of the strut. This study had a great impact on pursuing the current study. The pressure location in the combustor walls can be predicted by knowing the shock-impinging location in the combustor walls. This leads to Shock-boundary layer interaction [12-13]. To enhance mixing characteristics, more than one ramp or strut can be placed in the combustor simultaneously, leading to high total pressure loss [14-17].

Also, the thermoacoustic characteristics [18] impact the material structure which rises due to shock impingement. As more shocks are created, the more the acoustic characteristics dominate and the more the drag. In other cases, the fuel could be ejected directly from the strut by placing the injection hole between the cavity [19]. Numerical mixing studies were also done in this field using commercial CFD software to determine the degree of mixing [20].

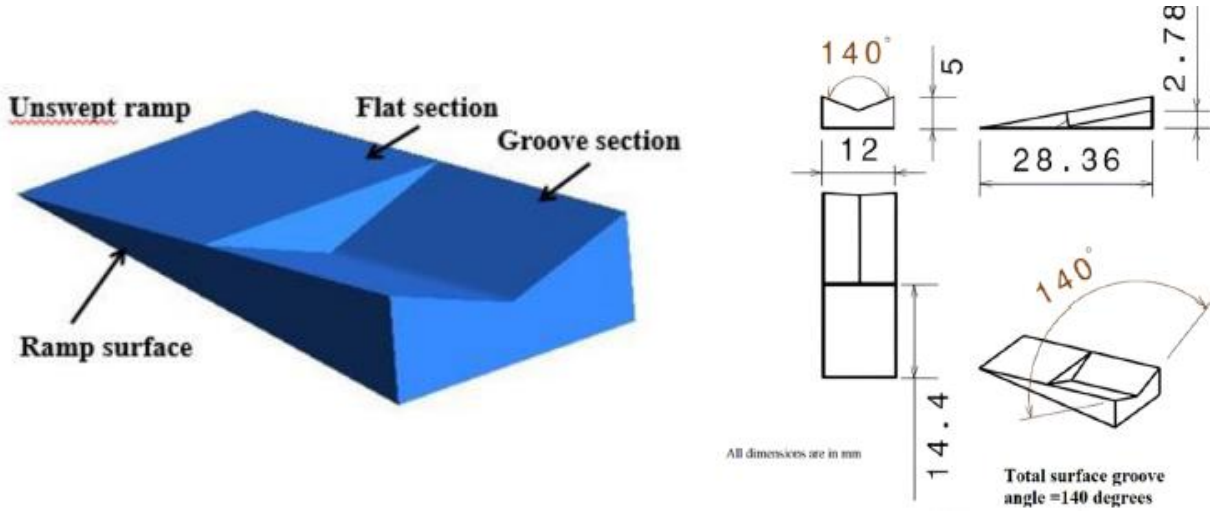

Fig. 2 Notch shaped strut and its dimensions

II. METHODOLOGY

The scramjet combustor uses high-temperature materials such as Heat-resistant alloys and ceramic matrix composites to withstand high temperatures. For making cold flow studies, SS304 material was used because it withstands high temperatures up to 1450°C and high pressures. Hence, the combustor was fabricated with SS304 alloy. The SS304 material of the required dimensions is trimmed in the shape of a cuboidal block. Then the block was given to wire cutting for fabricating the combustor model according to the dimensions of the jet facility. The fabricated combustor was drilled and bored at the required location for secondary injection. A mini settling chamber was made inside the combustor material by drilling tapped hole at the required depth and closing by using sealed screws leaving a gap inside for holding pressure. Then the ports are fixed at the holes to record total pressure. The inclinations of grooves are kept at 0˚ and 20˚ respectively as specified in [11].

The fabricated base plate model of the combustor was fixed with the existing combustor model using bolts and screws. The side walls of the combustor are made up of imported cast acrylic with a low refractive index for effective visualization of Schlieren images. The acrylic had a thickness of 8mm to withstand high transient pressure. The injector of diameter 1mm and length 50mm was made up of SS304 and the setup was fixed on the base plate of the combustor. The model was subsequently linked to an open jet facility operating at a pressure of 12 bar. An effective advisory light source (Sodium-vapour lamps) was set for the Schlieren setup. The resultant image of Schlieren was focused with a high-speed camera for generating effective photographs. The compressor was charged until its working pressure was reached by noting down pressure gauge readings.

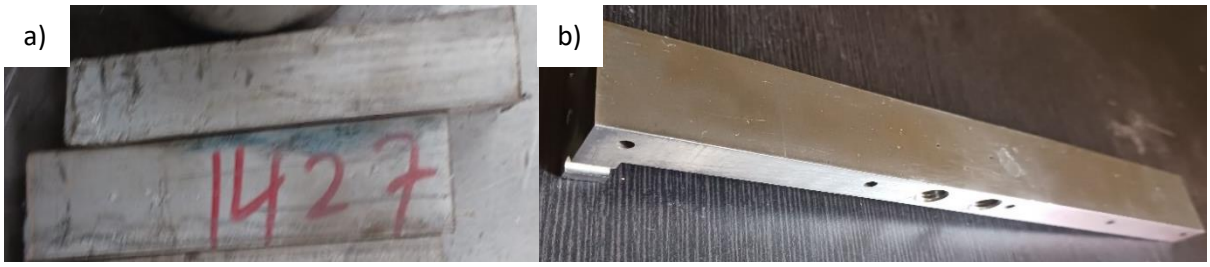

Figure **4** a) SS304 blocks b) SS Base plate of combustor after fabrication

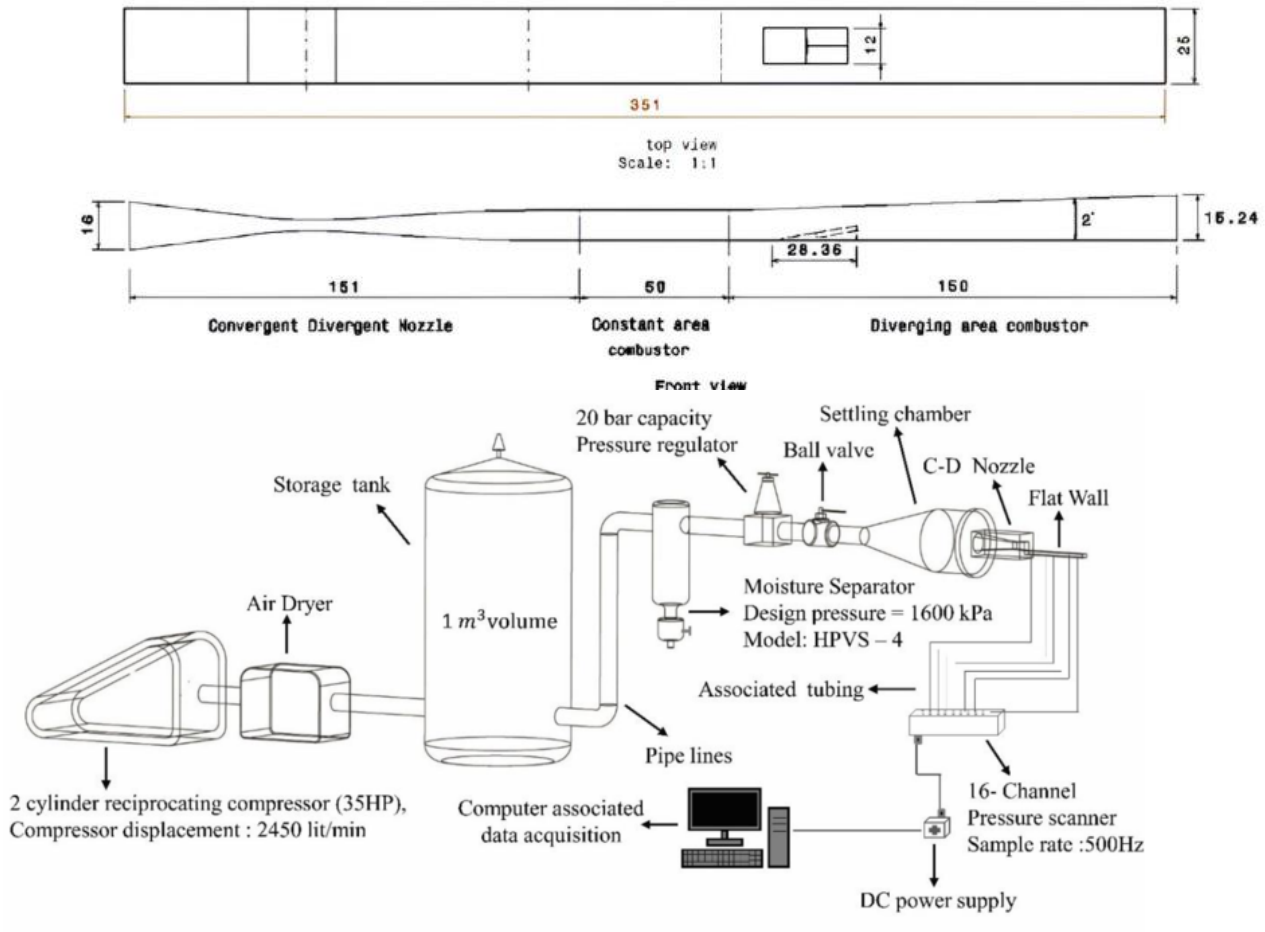

Figure 6. Schematic representation of Combustor

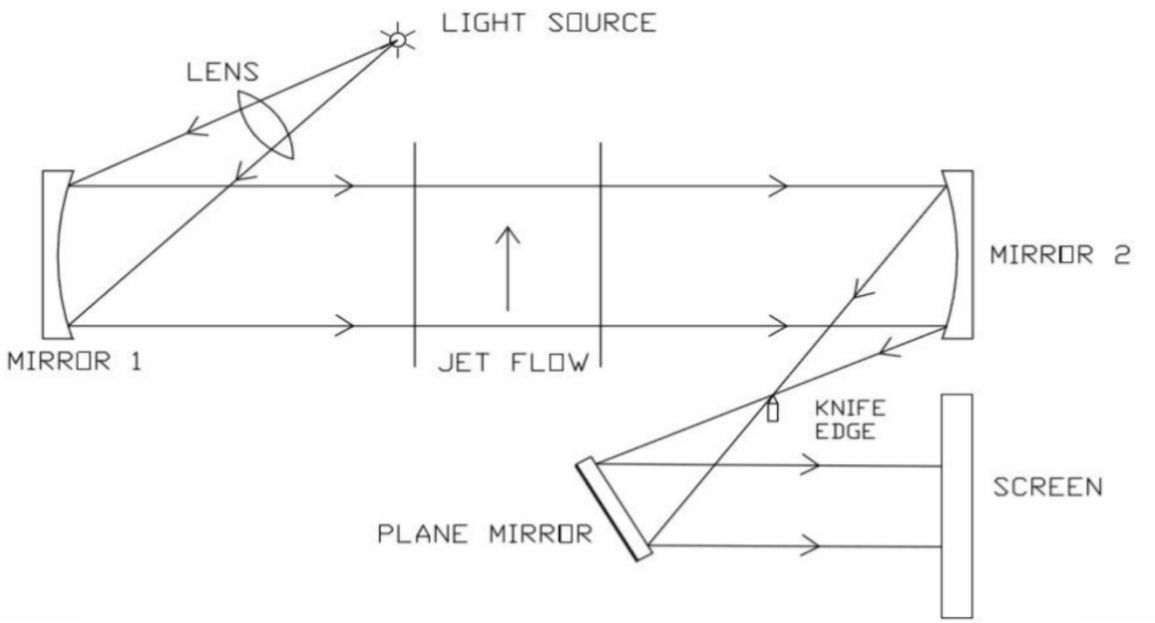

Fig. 7. Schematic representation of Schlieren system

The Illustration in Fig.7 was the schematic of the Schlieren system, which comprises two concave mirrors arranged in a Z-formation. A 200W halogen lamp serves as the light source, and each concave mirror has a focal length of 1100 mm, with a surface accuracy of λ/6. The other details were discussed briefly in [21]. The boundary conditions of this experiment are represented in the Table 1.

Type of boundary	**Boundary condition**	**Value**
Combustor Inlet	Total pressure	10 bar
Injector inlet in the presence of plane ramp	Total pressure	12 bar
Injector inlet in the presence of V-grooved strut	Total pressure	12 bar or 11 bar
Combustor inlet	Temperature	303 K
Combustor exit	Mach number	2.55
Injector inlet	Velocity	Sonic conditions

Table 1: Boundary Conditions

III. RESULTS AND DISCUSSION

The experiments were divided into two cases. In Case 1, the injector was positioned ahead of the ramp, while in Case 2, the injection occurred behind the ramp. The boundary conditions were selected according to the combustor exit Mach number. The flow field was examined by analyzing the Schlieren images for injection occurring at 30% of the ramp length ahead of the ramp, with a 20° strut, combustor inlet total pressure of 10 bar, and injection pressure of 12 bar is applied. Since the primary injection pressure is 10 bar, the secondary injection pressure must be greater than 10 bar to overcome the potential obstruction from the primary flow. The flow-field experiments were conducted for plane-ramp and grooved ramp at 12 bar injection pressure and the flow-field is

compared using flow visualization.

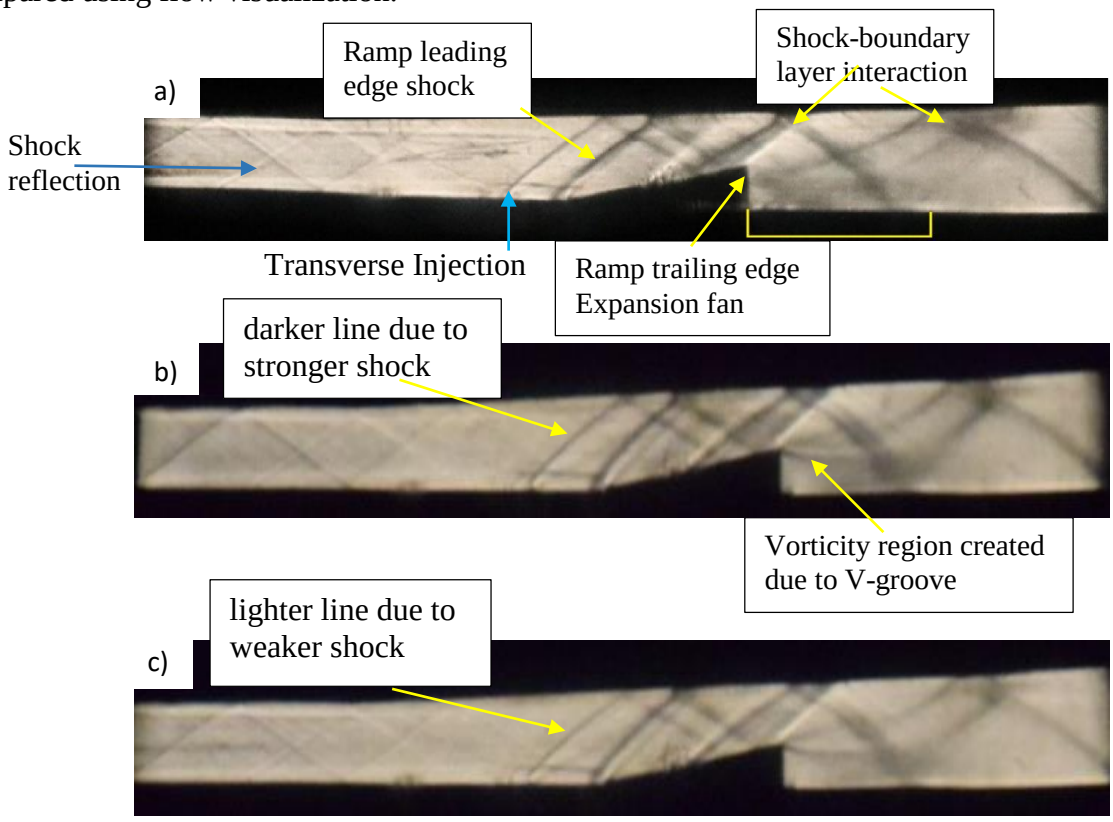

Fig. 8: Schlieren images of different flow-field in strut based combustor with injectior positioned at 30% of strut length ahead the strut a) Plane ramp with 12 bar injection pressure b) 20° grooved ramp with 12 bar injection pressure c) 20° grooved ramp with 11 bar injection pressure

The plane ramp configuration shown in Fig. 8 a) in which the injector was placed ahead of the strut. It can be observed that a normal shock was created at the place of injection. Due to shock reflection, the secondary flow gets turned to the recirculation region at the aft surface of the combustor. The dark area behind the strut shows the high-density region where the secondary fluid mixing region occurs. At the same time, there were many shock-boundary layer interactions at divergent sections of the combustor which may cause significant pressure loss and lead to flow separation.

The Schlieren representation of case 1 as depicted in Fig. 8 signifies that, the injection takes place ahead of the ramp. The position of the injector was at 30% of the strut length ahead or upstream of the strut. The total pressure of the combustor inlet was maintained at 10 bar. From Figure 8 it can be observed that there was no difference between the shock patterns at 12 bar Fig.(8b) and 11 bar Fig.(8c) injection. From [11] it was evident that the vortex strength was predominant within one ramp length behind the ramp. Hence, the transverse injection was done at 30% of the strut length. This shows that at higher pressures, the range of pressure of secondary injection does not significantly affect the shock patterns generated around the ramp. The shock patterns in Figure 8

can be seen curved behind the 20° grooved strut but the pattern was straight behind the plane ramp. This was due to the three-dimensional effect on the flow pattern projected in the two-dimensional Schlieren image.

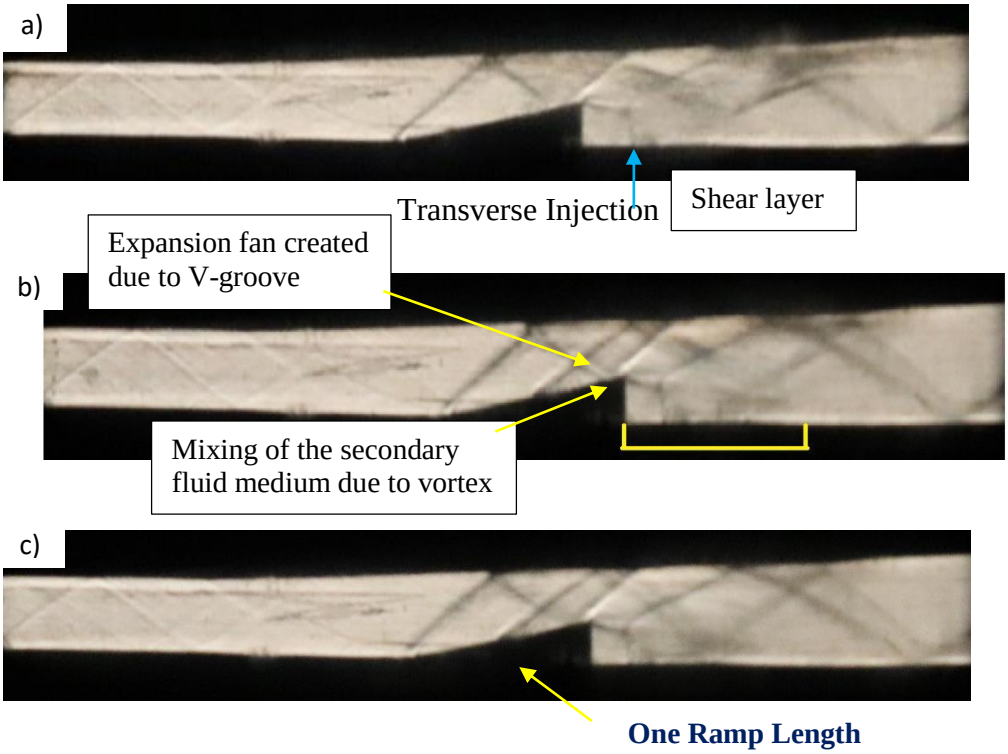

Fig. 9: Schlieren images of different flow-field in strut-based combustor with injector positioned at 30% of strut length behind the strut a) Plane ramp with 12 bar injection pressure b) 20° grooved ramp with 12 bar injection pressure c) 20° grooved ramp with 11 bar injection pressure

Similarly Figure 9 a) provides the Schlieren representation of case 2 in plane ramp configuration where the injection occurs behind the ramp. The position of the injector was at 30% of the ramp length behind the ramp. The shear layer of the plane ramp could be seen while the secondary medium encounters it. Due to its encounter, the mixing happens within the vortex region. The recirculation region could be seen clearly after the ramp till the injection. If the injector were positioned farther behind the strut, the shear layer might become relatively weaker, leading to reduced mixing. In this case, there was no difference between the shock patterns at 12-bar and 11-bar injection but the intensity changes. It indicates that, during high-pressure values, the variation in secondary injection pressure has minimal impact on the shock patterns formed around the ramp. The shock patterns observed in Fig. 10 a) and 10 b) can be seen curved behind the 20° grooved strut but the pattern was straight behind the plane ramp. **In the case of a plane ramp, there is no dimensional variation in the transverse direction. However, for the 20° notched ramp, the dimensional variation introduces a 3D relieving effect. Hence, the curved pattern of the shock was predominant due to 3D effects.**

IV. CONCLUSION

The experimental studies investigated the impact of secondary fluid injected in the transverse direction in a typical strut-based scramjet combustor. The present study used a plane strut and a typical V-grooved strut under different injection pressures. The experiments are divided into Case 1 for injection ahead of the strut and Case 2 for injection behind the strut. From the observations, it was predicted that, compared to the plane strut, the V-grooved strut generated more vorticity in the Z-direction under identical injection pressure. The V-groove created a three-dimensional vortex behind the strut leading to enhanced fluid mixing when injection occurred ahead of the strut. Under varying injection pressures, the shock patterns remain constant, with only the mass flow rate was changing. Thus, case 1 with a V-grooved strut at 11 bar injection could enhance combustion. However, In case 2, reverse flow was observed in the secondary fluid. In the plane ramp configuration, fluid was carried away from the recirculation zone which diminished the mixing phenomenon. In the V-grooved strut configuration, the fluid remains within the vortex region existing up to one strut length beyond the strut which enhanced the mixing. Therefore, case 2 for the V-grooved ramp could be advantageous for effective mixing, as it took place within the circulation zone, unlike case 1 and it was considered for enhancing the combustion efficiency. In future, the shock impact points will be determined which may be useful in recording wall pressure. Also, CFD simulation will be conducted to validate the experimental studies under different turbulent models and to quantify the degree of mixing.

ACKNOWLEDGEMENT

I would like to thank Madras Institute of Technology, Chennai for providing lab facilities for the present study. I thank NITTTR Chennai for providing technical help for the present study.

REFERENCES

1. Soni, R. K., & De, A. (2017). Investigation of strut-ramp injector in a Scramjet combustor: Effect of strut geometry, fuel and jet diameter on mixing characteristics. *Journal of Mechanical Science and Technology*, *31*, 1169-1179.
2. Manna, P., Behera, R., & Chakraborty, D. (2008). Liquid-fueled strut-based scramjet combustor design: a computational fluid dynamics approach. *Journal of Propulsion and Power*, *24*(2), 274-281.
3. Moorthy, J. V. S., Rajinikanth, B., Charyulu, B. V. N., & Rao, G. A. P. (2014). Effect of ramp-cavity on hydrogen fueled scramjet combustor. *Propulsion and Power Research*, *3*(1), 22-28.
4. Förster, F. J., Dröske, N. C., Bühler, M. N., von Wolfersdorf, J., & Weigand, B. (2016). Analysis of flame characteristics in a scramjet combustor with staged fuel injection using common path focusing schlieren and flame visualization. *Combustion and Flame*, *168*, 204-215.
5. Li, L. Q., Huang, W., Yan, L., Li, S. B., & Liao, L. (2018). Mixing improvement induced by the combination of a micro-ramp with an air porthole in the transverse gaseous injection flow field. *International Journal of Heat and Mass Transfer*, *124*, 109-123.

6. Li, L. Q., Huang, W., Fang, M., Shi, Y. L., Li, Z. H., & Peng, A. P. (2019). Investigation on three mixing enhancement strategies in transverse gaseous injection flow fields: A numerical study. *International Journal of Heat and Mass Transfer*, *132*, 484-497.
7. Zhang, Y., Liu, W., Wang, B., & Sun, M. (2016). Effects of micro-ramp on transverse jet in supersonic crossflow. *Acta Astronautica*, *127*, 160-170.
8. Li, C., Zhao, X., Xia, Z., Ma, L., & Chen, B. (2019). Influence of the vortex generator on the performance of solid rocket scramjet combustor. *Acta Astronautica*, *164*, 174-183.
9. Segal, C. (2009). *The scramjet engine: processes and characteristics* (Vol. 25). Cambridge University Press.
10. Dimotakis, P. E. (1986). Two-dimensional shear-layer entrainment. *AIAA journal*, *24*(11), 1791-1796.
11. Gnanasekaran, J., & Sridhar, B. T. N. (2024). Investigation on compression ramp with surface V-groove for scramjet combustor. *Journal of the Brazilian Society of Mechanical Sciences and Engineering*, *46*(9), 570.
12. Bezerra, Í. S., Araújo, P. P., Souza, S. I., Marinho, G. S., & Toro, P. G. (2024). Influence of the hydrogen transverse injection mode in a scramjet combustor performance. *International Journal of Hydrogen Energy*, *53*, 1269-1284.
13. Jiao, G., Song, W., & Zeng, X. (2024, June). Experimental study on dynamic characteristics of wall pressure in supersonic combustor of kerosene fuel. In *Journal of Physics: Conference Series* (Vol. 2772, No. 1, p. 012011). IOP Publishing.
14. Athithan, A. A., Jeyakumar, S., Sczygiol, N., Urbanski, M., & Hariharasudan, A. (2021). The combustion characteristics of double ramps in a strut-based scramjet combustor. *Energies*, *14*(4), 831.
15. Huang, Z., Rong, C., Liu, H., Li, L., & Zhang, B. (2024). Investigation on the effect of coupling factors on combustion performance of a hydrogen fueled two-strut scramjet combustor. *International Journal of Hydrogen Energy*, *80*, 1103-1115.
16. Choubey, G., Solanki, M., Patel, O., Devarajan, Y., & Huang, W. (2023). Effect of different strut design on the mixing performance of H2 fueled two-strut based scramjet combustor. *Fuel*, *351*, 128972.
17. Chaubey, G., Dalal, K., Chavda, P., & Huang, W. (2024). Three-dimensional CFD analysis of two-strut assisted scramjet combustor. *International Journal of Fluid Mechanics Research*, *51*.
18. Nair, P. P., Ananthu, J. P., & Narayanan, V. (2024). Effect of jet splitting using passive strut on the performance and thermoacoustic characteristics of a scramjet combustor. *Physics of Fluids*, *36*(8).
19. Quan, F., Chang, J., Kong, C., Lv, C., & Wu, G. (2024). Research on mixing characteristics of scramjet combustor equipped with strut injector. *Applied Thermal Engineering*, *236*, 121527.
20. Kireeti, S. K., Ravikiran Sastry, G., & Gugulothu, S. K. (2024). Numerical investigation on implication of innovative hydrogen strut injector on performance and combustion characteristics in a scramjet combustor. *International Journal of Turbo & Jet-*

Engines, *40*(s1), s43-s57.

21. Sureshkumar, A., & Sridhar, B. T. N. (2020). Axial flow development characteristics of circular and triangular supersonic jets in the presence of an annular coflow at large separation distance. *Proceedings of the Institution of Mechanical Engineers, Part G: Journal of Aerospace Engineering*, *234*(3), 804-817.